# Water desalination via pressure-driven distillation with chlorine-resistant and large-area polymeric membranes

Environmental Science and Technology Letters

Duong T. Nguyen<sup>1</sup>, Kian P. Lopez<sup>2</sup>, Sangsuk Lee<sup>1</sup>, Jongho Lee<sup>4</sup>, Mark Hernandez<sup>1</sup>, and Anthony P. Straub<sup>1,5</sup>\*

<sup>&</sup>lt;sup>1</sup>Department of Civil, Environmental and Architectural Engineering, University of Colorado Boulder, Boulder, Colorado 80309, USA,

<sup>&</sup>lt;sup>2</sup>Department of Chemical and Biological Engineering, University of Colorado Boulder, Boulder, Colorado 80309, USA,

<sup>&</sup>lt;sup>3</sup>Department of Civil Engineering, University of British Columbia, Vancouver, British Columbia V6T 1Z4, Canada.

<sup>&</sup>lt;sup>4</sup>Material Science and Engineering Program, University of Colorado Boulder, Boulder, Colorado 80309, USA

<sup>\*</sup> Corresponding author: Anthony Straub, Email: Anthony.Straub@colorado.edu

#### **ABSTRACT**

Pressure-driven distillation is a separation process in which hydraulic pressure is used to drive water vapor transport across an air-trapping porous hydrophobic membrane. Current development of pressure-driven distillation is limited by a lack of robust, large-area membranes. Here, we report desalination using pressure-driven vapor transport through scalable polymeric polytetrafluorethylene membranes. The membranes showed pressure-driven water flow with nearcomplete rejection of sodium chloride (greater than 99%) under hydraulic pressures of up to 10.3 bar. Membrane structure, surface chemistry, and desalination performance were found to be unaffected by doses of sodium hypochlorite up to 3,000 ppm h. Flux decline due to biofouling from Pseudomonas aeruginosa bacterium was effectively mitigated using chlorine. Membranes also exhibited high temperature resilience, with operation up to 60 °C. Overall, this work demonstrates the use of large-area polymeric materials in pressure-driven distillation and highlights key advantages in chlorine and heat tolerance.

13

14

15

1

2

3

4

5

6

7

8

9

10

11

12

**Keywords**: Pressure-driven distillation, desalination, vapor transport, biofouling, hydrophobic porous membrane

16

17

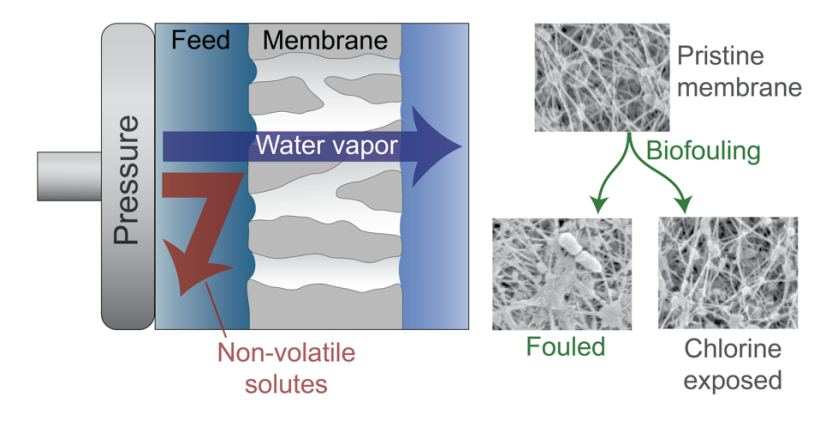
18

**Synopsis**: Water desalination using pressure-driven distillation is demonstrated with large-area membranes that can be effectively cleaned using chlorine.

19

20

TOC Art



22

# INTRODUCTION

Water reuse and desalination are essential to relieve global water scarcity by purifying water from sustainable, non-traditional sources.<sup>1,2</sup> Reverse osmosis (RO) is a widely used process in desalination and water reuse treatment trains because it offers energy efficiency, scalability, and reliable removal of key contaminants (e.g., dissolved ions and organic carbon).<sup>3–5</sup> However current RO membrane materials suffer from critical shortcomings. Notably, RO membrane materials readily degrade when exposed to free chlorine commonly used in water reuse treatment trains.<sup>6,7</sup> As a result, RO membranes cannot be easily cleaned and costly dechlorination steps must often be employed.<sup>8</sup> RO membranes also suffer from poor rejection of small neutral compounds, meaning that secondary treatment steps, such as advanced oxidation, ion exchange, or a second RO pass, are required to remove boron, certain disinfection byproducts, and other harmful pollutants.<sup>9–11</sup>

Pressure-driven distillation (PD) is an emerging process that can achieve higher selectivity and oxidation resistance than current RO systems. PD uses applied hydraulic pressure to drive vapor transport through an air-trapping porous hydrophobic membrane. In operation, PD is similar to RO in that it uses applied pressure to drive water flow, and PD membrane modules could eventually directly replace RO modules in a water treatment train. The key advantages of PD compared to RO are that it offers higher rejection of certain contaminants (specifically, non-volatile contaminants) and uses membrane materials that resist oxidation and heat. PD is also similar to membrane distillation (MD) in that transport occurs in the vapor phase through porous hydrophobic membranes; the main difference between PD and MD is that pressure is the driving force in PD rather than temperature, making PD a more energy efficient method of separation. Modeling work has shown that the energy efficiency of PD is likely similar to that of RO since both are driven by hydraulic pressure and detrimental heat transfer effects in PD are minimal for all realistic membrane properties. Significance of the properties of PD are minimal for all realistic membrane properties.

Despite the potential benefits of PD in desalination and other separations, few studies have experimentally investigated the process, in part due to the challenge of operating air-trapping membranes at pressures above 5 bar without wetting. Those studies that have been conducted have gleaned important insights on the process, showing that PD is experimentally viable; that PD membranes can reach water permeabilities comparable to RO membranes; and that PD can highly reject boron, urea, and other contaminants. 12,17,18 However, prior studies have relied on expensive exotic materials, such as hydrophobic porous alumina and carbon fiber, with small membrane areas

(less than 6.5 cm<sup>2</sup>). Such materials are not representative of the scalable, flexible membranes typically required for large-scale desalination. To make PD viable for seawater desalination or wastewater reuse, there is an urgent need for large-area, robust, and cost-effective membranes that handle high applied pressure without pore wetting.

In this study, we demonstrate the pressure-driven distillation process for desalination using large-area polytetrafluoroethylene (PTFE) membranes. Desalination performance of the membranes is investigated at high hydraulic pressures, and rejection of salts is demonstrated for a wide range of operating pressures and temperatures. The effect of chlorine on desalination performance, membrane structure, and chemical bonding is investigated. Fouling mitigation using chlorine is also studied using *Pseudomonas aeruginosa* as a surrogate biofilm-forming bacterium. Overall, this work shows the use of scalable polymeric membranes in PD and highlights potential advantages of PD in chlorine tolerance and biofouling mitigation.

# MATERIALS AND METHODS

Membranes and test cells. Commercial polytetrafluoroethylene (PTFE) membranes with a 20 nm nominal pore size were obtained from Pall Corporation (PTFE-002, NY, USA). Thin-film composite (TFC) polyamide membranes for seawater desalination were purchased from Dupont (SW30-XLE, DE, USA) to compare performance. Desalination behavior of the membranes was examined in a small-scale test cell and a larger scale crossflow system. The small-scale dead-end system held membranes with a diameter of 13 mm and an active area of 84.9 mm<sup>2</sup>. The larger scale crossflow system had an effective membrane area of 15.4 cm<sup>2</sup> and operated with a crossflow velocity of 65 cm min<sup>-1</sup>.

Measurement of liquid entry pressure and desalination performance. The liquid entry pressure (LEP) of the membrane was determined by gradually increasing hydraulic pressure in the feed water and recording the applied pressure at which liquid water starts permeating through the membrane. In desalination testing, a feed solution of 50 mM NaCl was used. Hydraulic pressures were applied ranging from 3.45 to 10.3 bar. A uniform fixed temperature was maintained in the entire system (feed and permeate reservoir) using a water bath. Water flux was monitored via the increase in water volume in the permeate and the loss of water volume in the feed. Electrical conductivity of the collected feed and permeate samples were measured using a calibrated

conductivity meter (Oakton CON2700, MA, USA) and corrected for dilution in the permeate channel to determine the apparent NaCl rejection.

Chlorine exposure and biofouling experiments. Exposure of PTFE membranes to chlorine was conducted using a stirred 1000 ppm sodium hypochlorite solution for 3 h under pH 4. The membrane was fixed to the wall of a glass beaker so only the active PTFE layer was exposed to chlorine solution. Static fouling of PTFE membranes and TFC-RO polyamide membranes was performed with pure cultures of *Pseudomonas aeruginosa* (ATCC 15442). 19,20 PTFE and TFC RO polyamide membranes were installed in the membrane cell leaving solely the feed side of the membrane exposed to the bacteria suspensions, following a similar method as previous biofouling work. 3 mL of the diluted bacteria suspensions with a concentration of 1.2 × 106 colony-forming units per milliliter (CFU mL-1) were in contact with the membrane active layer for 3 h. After discarding the suspensions, the membrane was mildly rinsed with sterile phosphate buffer to detach cell debris on the membrane surface. Fouling behavior of chlorine-exposed samples was investigated where 1000 ppm sodium hypochlorite solution at pH 4 with bacteria suspension was in contact with the membranes for 3 h. Desalination performance of the membranes was examined using a feed solution of 0.1 M phosphate buffer and a hydraulic pressure of 10.3 bar.

### **RESULTS AND DISCUSSION**

**Polymeric membranes resist wetting at high pressures.** Pressure-driven distillation (PD) uses applied hydraulic pressure to drive water vapor transport through an air-trapping hydrophobic membrane (Figure 1A). Membranes used in PD must be able to withstand high applied pressure without liquid water penetration into the membrane pores. The liquid entry pressure (LEP) of a pore can be estimated using Young-Laplace theory:<sup>22,23</sup>

$$LEP = -\frac{2\beta\gamma\cos\theta}{r} \tag{1}$$

where  $\gamma$  is the surface tension of the liquid-vapor interface,  $\theta$  is the intrinsic liquid contact angle, r is the pore radius, and  $\beta$  is a pore geometry factor accounting for noncylindrical pores. From Young-Laplace theory, it is evident that membranes operating at high pressure must have a small pore size (less than 100 nm) and high hydrophobicity.

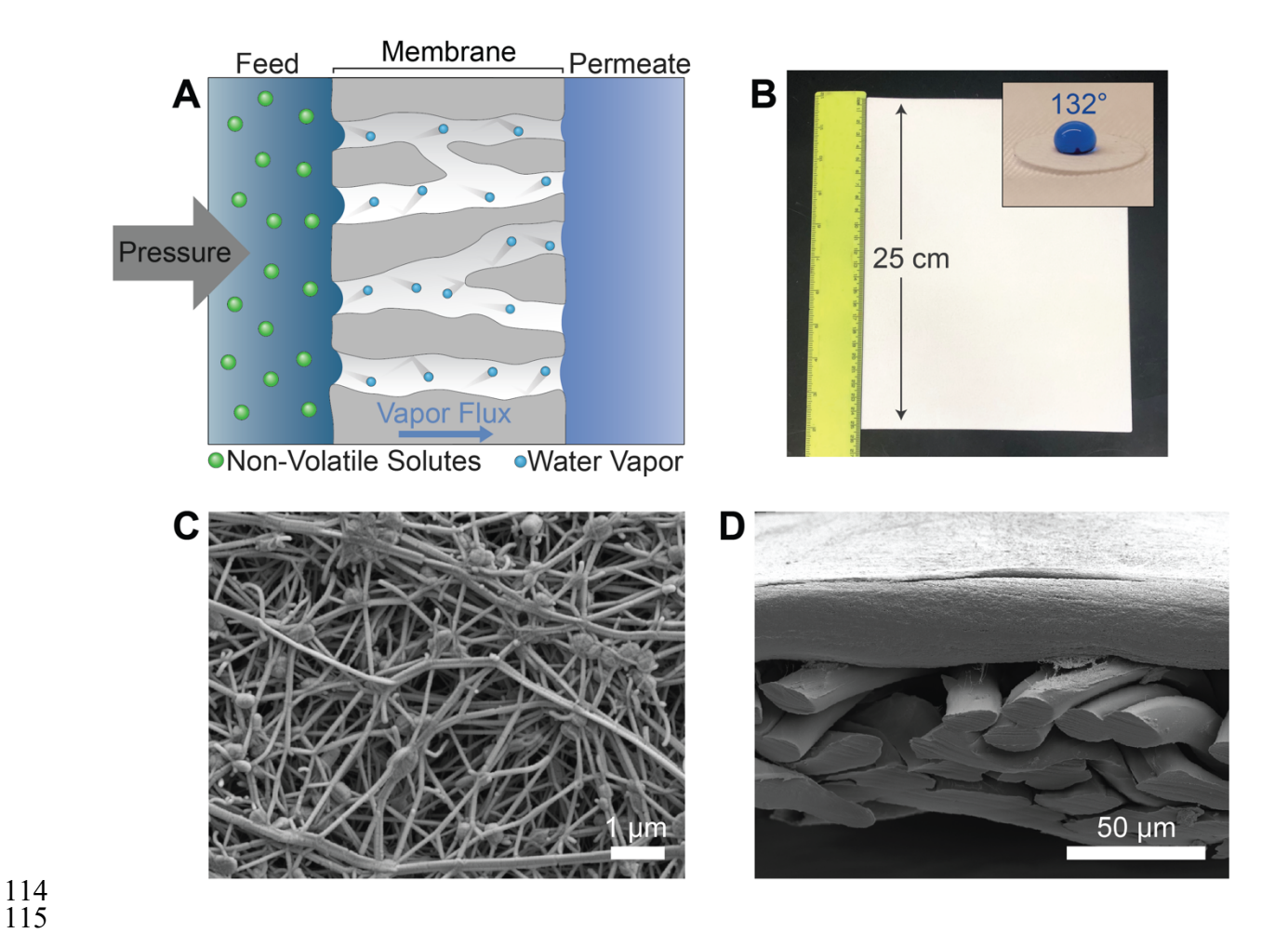


**Figure 1.** (A) Schematic diagram of water vapor transport across porous hydrophobic membranes driven by hydraulic pressure difference. (B) Photograph of the polytetrafluorethylene (PTFE) membrane sheet with the contact angle of liquid water on the surface shown in the inset. (C and D) Top-down and cross-section scanning electron microscopy (SEM) images of the PTFE membrane.

Hydrophobic porous PTFE membranes were selected for testing because (1) they are already commercially produced in large sheets (Figure 1B); (2) they are highly hydrophobic with an observed contact angle of  $132\pm1.6^{\circ}$  (Figure 1B, inset); and (3) they have a small 20 nm nominal pore size that can facilitate a high LEP. Scanning electron microscopy (SEM) images of the membrane showed properties consistent with those observed in the prior literature including an approximately 43  $\mu$ m-thick PTFE layer, an unwoven polyester backing layer, a total membrane thickness of approximately 136  $\mu$ m, and a porosity of 77% (Figure 1C, D).<sup>24</sup>

The liquid entry pressure (LEP) was measured by sequentially increasing the pressure applied across the membrane. Triplicate measurements observed a liquid entry pressure 13.8 bar, an LEP value higher than most hydrophobic membranes which typically wet at pressures less than 5 bar. From this LEP, we estimate that the largest membrane pores are approximately 65 nm in diameter (assuming an intrinsic contact angle of 108°).<sup>25</sup> The maximum operating pressure of the PTFE membrane would allow for desalination of saline water with an osmotic pressure of up to 13.8 bar which corresponds to a total dissolved solids (TDS) concentration of approximately 3 g L<sup>-1</sup>; thus, commercial PTFE membranes would be suitable for the treatment of certain brackish waters or saline wastewater effluent.

Desalination is observed via pressure-driven distillation. Desalination performance of the PTFE membrane coupon was examined in dead-end testing using a feed solution of 50 mM NaCl and applied hydraulic pressures ranging from 3.45 to 10.3 bar (Figure 2). The measured water flux increased monotonically from 0.034 to 0.13 L m<sup>-2</sup>h<sup>-1</sup> when increasing applied pressure from 3.45 to 10.3 bar at a uniform system temperature of 30 °C (the temperature of the test cell, feed reservoir, and permeate reservoir were all maintained constant). Water flux further increased when increasing the uniform temperature of the system, reaching 0.34 L m<sup>-2</sup>h<sup>-1</sup> with a hydraulic pressure of 10.3 bar and a uniform system temperature of 60 °C. In all tests, we observed higher than 99.5% NaCl rejection for the duration of experiments, indicating that liquid water does not intrude into the membrane pores and transport in the process occurs in the vapor phase. Testing with a larger area crossflow membrane cell (15.4 cm<sup>2</sup>) showed consistent water flux values (less than 15% deviation) and high salt rejection (Figure S1).

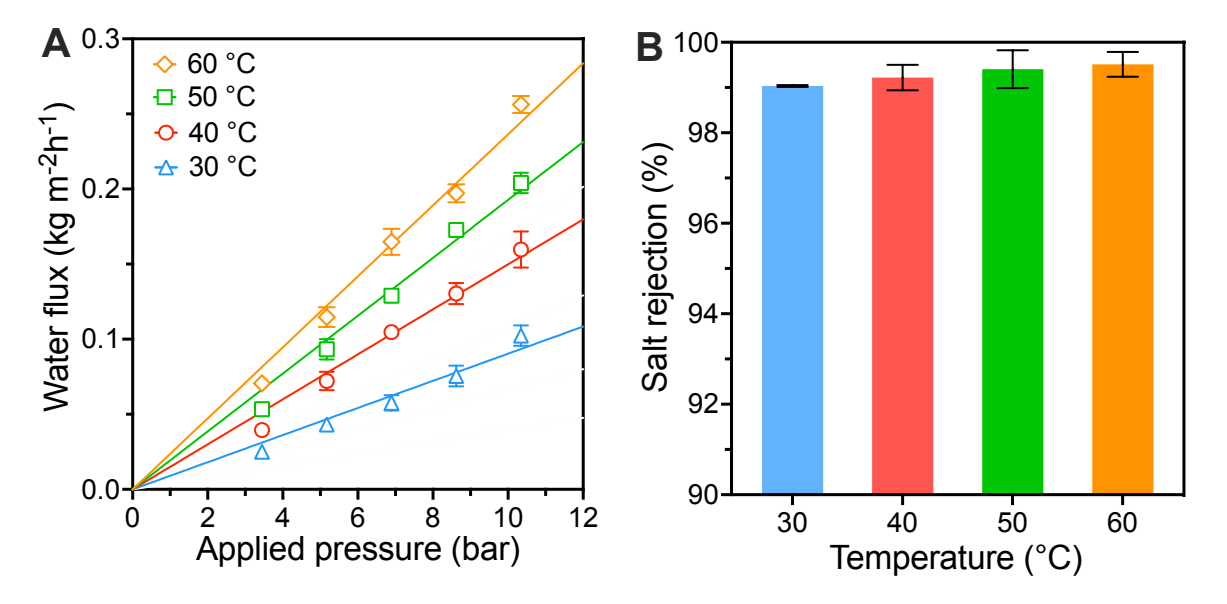


**Figure 2.** Desalination performance of PTFE membranes. (A) Water flux across the PTFE membrane as a function of applied pressure and temperature. 50 mM NaCl was used as the feed solution. The hydraulic pressure of feed side was varied from 3.45 to 10.3 bar. The uniform temperature of the system (feed reservoir, test cell, and permeate reservoir) was adjusted from 30 to 60 °C using a water bath. Lines are linear fits for each temperature. (B) Salt rejection of PTFE membranes taken from four different experiments using a feed water of 50 mM NaCl, a hydraulic pressure of 10.3 bar, and temperatures of 30 to 60 °C.

Measured desalination rates showed agreement with theoretical simulations by the Dusty-Gas model. Water mass flux across the membrane,  $J_w$ , can be expressed as the product of the evaporation rate difference between the feed and permeate interfaces,  $\Delta S$ , and membrane porosity,  $\varepsilon$ , divided by the total resistances experienced as water traverses the pore,  $\Sigma R$ :13,14

$$J_w = \varepsilon \frac{\Delta S}{\Sigma R} \cong B_w \Delta P_v \quad (2)$$

This relationship can be simplified to the product of the partial vapor pressure difference across the membrane,  $\Delta P_{\nu}$ , and the vapor permeability coefficient,  $B_{\nu}$ , a proportionality factor which relates flux to a partial vapor pressure difference and includes contributions from both transmission and interfacial resistances (see full derivation in the Supporting Information). The partial vapor pressure at a giving air-liquid interface,  $P_{\nu}$ , is expressed as a function of temperature (T), concentration (C), and hydraulic pressure  $(P_h)$  using the Kelvin equation and Raoult's Law:<sup>22</sup>

171 
$$P_{v}(T, C, P_{h}) = P_{v,0}(T)a_{w}(C)\exp\left(\frac{P_{h}V_{m}}{R_{q}T}\right)$$
 (3)

where  $a_w(C)$  is the water activity as a function of solute concentration,  $V_m$  is the molar volume of liquid water,  $R_g$  is the universal gas constant, and  $P_{v,0}$  is the equilibrium vapor pressure at the temperature, T defined by the Antoine equation. Using full simulations of the water flux that account for concentration polarization and temperature polarization (see Supporting Information), we found less than 20% deviation and coefficients of determination greater than 0.9 between experiments and models using measured membrane properties without any fitting parameters (Figure S2). The strong agreement between experimental water fluxes and those predicted by theory indicate the validity of transport models for membranes with non-ideal pore structures. The models also allow us to understand methods to increase the water flux, which was relatively low in our experimental observations. Notably, the water flux can be substantially increased by decreasing the thickness of the membrane hydrophobic layer from the current thickness of approximately 43  $\mu$ m to values less than 500 nm. <sup>12,26</sup> The importance of thin hydrophobic layers in improving flux was also shown in our experimental work using custom-made ceramic membranes, where a 119 nm thick air layer allowed for water permeabilities exceeding 1.3 kg m  $^2$ h- $^1$ bar- $^1$ .

Chlorine treatment mitigates biofouling. The ability to tolerate chlorination was investigated by immersing PTFE membranes in 1000 ppm sodium hypochlorite solution at pH 4 for 3 h prior to desalination testing. After chlorine exposure, the observed salt rejection of the membranes was unaffected by testing and remained greater than 99% (Figure 3A). The water flux of the chlorine-exposed membrane also deviated less than 10% from that of the pristine membrane. FTIR analysis showed that characteristic peaks at the transmittances of 1237 and 1125 cm<sup>-1</sup> corresponding to -CF<sub>2</sub> symmetric and asymmetric stretching vibrations were maintained with no significant change in peak intensity after chlorination, implying the chemistry of PTFE membranes remains stable after chlorination (Figure 3B). We also observed a less than 5% change in average water contact angle of PTFE membranes from 132 to 128° after chlorine exposure (Figure 3B, inset). The chlorine resistance of PTFE is consistent with our understanding that the material is not affect by chlorine radicals and other strong oxidants.<sup>27,28</sup>

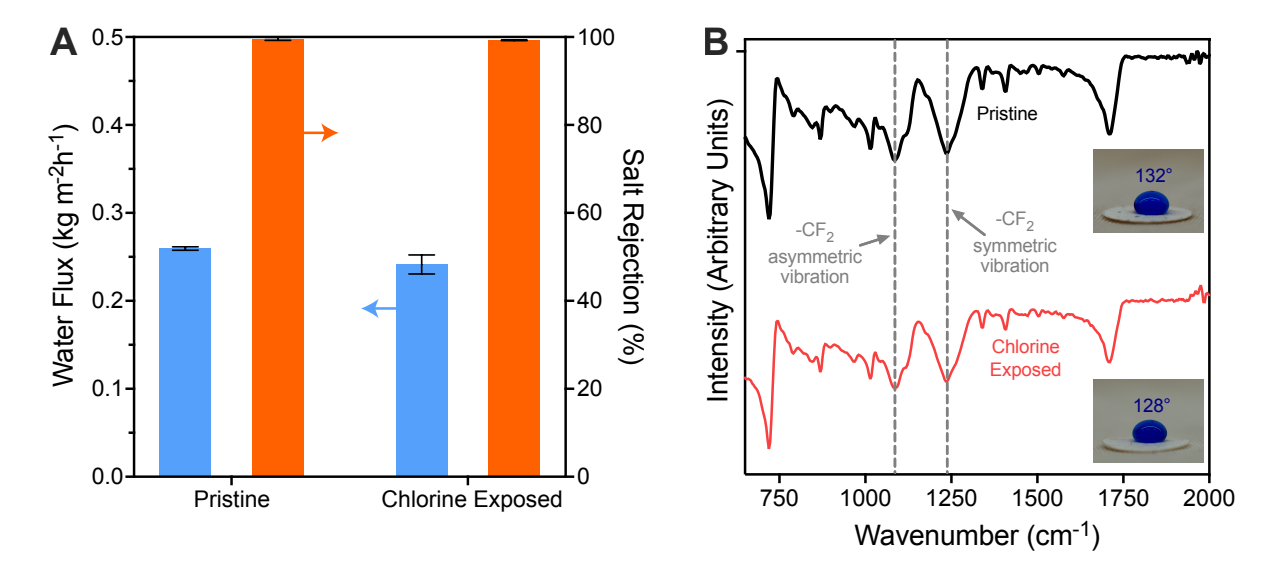


**Figure 3.** Chlorine tolerance of the PTFE membrane. (A) Water flux (blue) and salt rejection (orange) of PTFE membranes before and after exposure to 1000 ppm chlorine for 3 h at pH 4. Error bars show the standard deviation for duplicate measurements with two separate membrane coupons. (B) FTIR spectra and water contact angle of pristine and chlorine-exposed PTFE membranes.

The impact of biofouling on desalination performance was investigated using feedwaters dosed with live P. aeruginosa biofilm forming bacterium with a concentration of  $2 \times 10^6$  colony-forming units per milliliter (CFU mL<sup>-1</sup>). Fouling performance and fouling mitigation using chlorine was probed using PTFE membranes in PD and commercial TFC RO membranes as a control. After 3 h of static biofouling, the water flux of the PTFE membrane was reduced by 69% (Figure 4A). The TFC RO membrane control after 3 h of static biofouling showed an 81% decrease in water flux and a reduction in salt rejection to 78%, possibly due to increased water transport resistances and cake-enhanced concentration polarization. SEM imaging of the fouled PTFE membrane confirmed the presence of biofilm forming bacteria on the surface (Figure 4B, C).

Direct chlorination of the bacteria feed solutions on the membrane surface prevented biofouling of PTFE membranes with less than 5% water flux decline. After chlorine exposure, bacteria were absent on the PTFE membrane surface as confirmed by SEM imaging and no significant changes in surface morphology and structure of PTFE membranes were observed after chlorine exposure (Figure 4D). Attempts to mitigate fouling by direct chlorination of TFC RO membranes resulted in a loss of salt rejection (decrease from higher than 99% salt rejection to 64%), which is attributed

to the damage of polyamide selective layer by chlorine exposure.<sup>6</sup> Thus, the chlorine tolerance of PTFE membrane in PD enabled fouling mitigation not possible with conventional polymeric RO membranes.

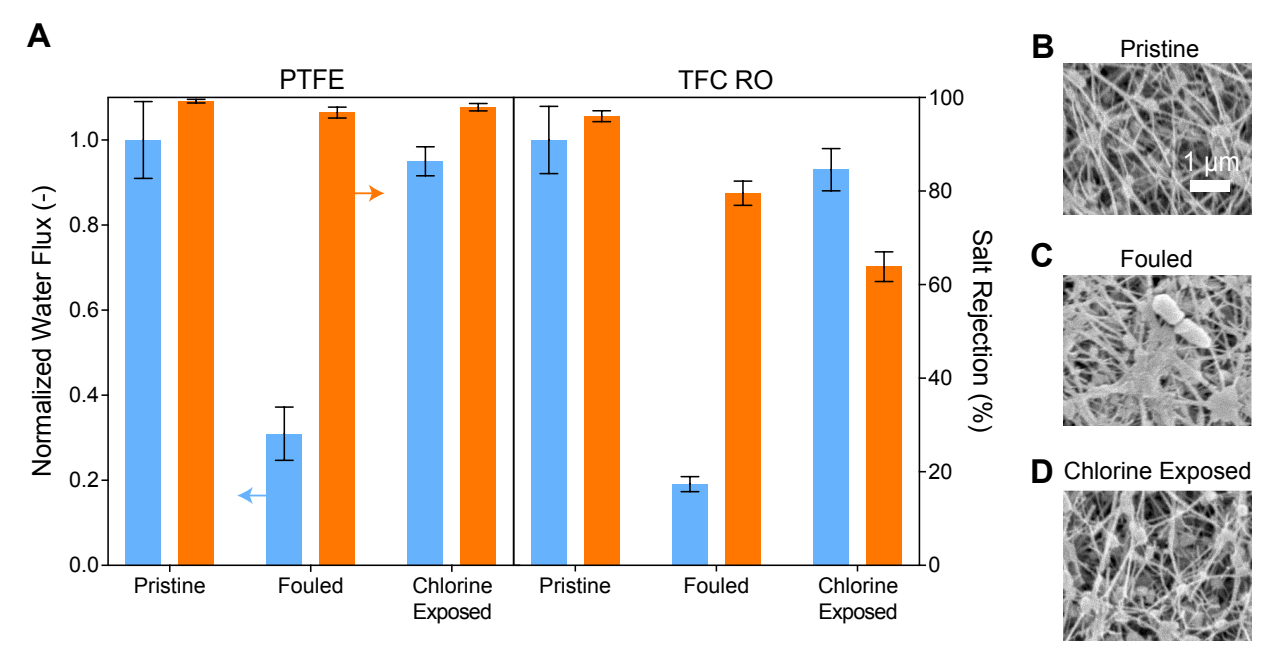


**Figure 4.** Biofouling behavior of PTFE membranes and mitigation by chlorine treatment. (A) Water flux (blue) and salt rejection (orange) of pristine PTFE and TFC RO membranes, membranes fouled with live *P. aeruginosa*, and membranes fouled with a chlorinated *P. aeruginosa* feed solution. Error bars show the standard deviation for duplicate measurements with two membrane coupons. (B-D) SEM images of the top surface of the pristine PTFE membrane, the membrane after biofouling, and the membrane after fouling with a feed solution dosed with 1000 ppm chlorine at pH 4.

Implications for membrane-based desalination. Pressure-driven water desalination using large-area polymeric PTFE membranes was demonstrated in this work. The PTFE membranes showed water vapor fluxes consistent with vapor transport theory and demonstrated high rejection (above 99%) of sodium chloride salts. Membranes were able to exhibit desalination performance in a crossflow membrane system with a 15.4 cm<sup>2</sup> area. After chlorination, PTFE membranes show neither compromises in desalination performance nor changes in structural and chemical integrity. The tolerance of PTFE membranes toward chlorine at exposures up to 3,000 ppm h enabled chlorine cleaning to prevent flux decline due to biofouling. PD membranes were also found to be

able to operate effectively at temperatures up to 60 °C, an advantage compared to polymeric RO membranes which are known to fail at temperatures above 45 °C.<sup>29</sup>

Although this work has demonstrated the promise of large-area membranes with chlorine tolerance for PD, further work is needed to improve membrane performance. A critical shortcoming of the commercial PTFE membranes in this work is that they demonstrate water permeabilities that are 1–2 orders of magnitude lower than conventional membranes used in RO. Models validated in this study and recent experimental work indicate that making the air layer of the membrane thinner (less than 500 nm) will result in higher permeabilities that are competitive with those of current RO membranes.<sup>12</sup> Future development of industrial-scale desalination modules with areas greater than 10 m<sup>2</sup> in spiral wound, hollow fiber, or flat sheet configurations is also essential to enable PD systems with a high membrane packing density.<sup>30,31</sup> In these modules, hydrophobic membrane materials that do not rely on fluorine-based chemistry should also be explored to mitigate the potential release of per- and polyfluoroalkyl substances. Air-trapping membranes used for PD are highly selective towards non-volatile contaminants but will likely allow compounds with relatively high volatility to pass through, and further investigations into contaminant rejection are needed.<sup>32</sup> Overall, this work demonstrates the promise of large-scale polymeric membranes in PD and highlights the need for continued membrane and process development on this emerging membrane process.

#### **ACKNOWLEDGMENTS**

The authors are grateful to financial support from the National Science Foundation under Award Number CBET 2227273 and from the Bureau of Reclamation, Department of Interior, via DWPR Agreement R22AC00425. We appreciate the funding from National Science Foundation Industry/University Cooperative Research Center for Membrane Science, Engineering and Technology (MAST) at the University of Colorado Boulder (UCB, award number, IIP 1624602). D.T.N is thankful to the support from the WateReuse Association for the 2021 Martha Hahn Memorial Scholarship and the North American Membrane Society for the 2021 Student Fellowship. K.P.L appreciates the National Aeronautics and Space Administration (NASA) for the Space Technology Graduate Research Opportunity (NSTGRO) fellowship. We also thank Pall and Danaher Corporation for providing membrane samples for coupon-scale and large-scale testing. We appreciate Dr. Edo Bar-Zeev at Ben-Gurion University, Dr. Lucas McIntosh at 3M, Dr. Uwe

- 273 Beuscher at Gore for helpful discussions on fouling characterization, membrane design, and
- 274 membrane testing. We acknowledge the University of Colorado Boulder Department of Chemistry
- for their assistance with FTIR and the Colorado Shared Instrumentation in Nanofabrication and
- 276 Characterization Laboratory for their help with SEM.

278

#### SUPPORTING INFORMATION AVAILABLE

Detailed information on measurements of desalination performance, preparation of bacterial cultures, membrane characterization, theoretical modeling of water vapor transport, desalination performance of large-area membrane (Figure S1), and agreement between experimental water flux and vapor transport simulations (Figure S2). This material is available free of charge via the Internet at http://pubs.acs.org.

279

280

# NOTE

The authors declare no competing financial interest.

282

283

#### REFERENCES

- 284 (1) Elimelech, M.; Phillip, W. A. The Future of Seawater Desalination: Energy, Technology, and the Environment. *Science* **2011**, *333* (6043), 712–717. https://doi.org/10.1126/science.1200488.
- 287 (2) Uliana, A. A.; Bui, N. T.; Kamcev, J.; Taylor, M. K.; Urban, J. J.; Long, J. R. Ion-Capture 288 Electrodialysis Using Multifunctional Adsorptive Membranes. *Science* **2021**, *372* (6539), 289 296–299. https://doi.org/10.1126/science.abf5991.
- 290 (3) Lin, S.; Elimelech, M. Staged Reverse Osmosis Operation: Configurations, Energy Efficiency, and Application Potential. *Desalination* **2015**, *366*, 9–14. https://doi.org/10.1016/j.desal.2015.02.043.
- 293 (4) Shaffer, D. L.; Yip, N. Y.; Gilron, J.; Elimelech, M. Seawater Desalination for Agriculture 294 by Integrated Forward and Reverse Osmosis: Improved Product Water Quality for 295 Potentially Less Energy. *J. Membr. Sci.* **2012**, *415–416*, 1–8. 296 https://doi.org/10.1016/j.memsci.2012.05.016.
- 297 (5) Nickerson, T. R.; Antonio, E. N.; McNally, D. P.; Toney, M. F.; Ban, C.; Straub, A. P. Unlocking the Potential of Polymeric Desalination Membranes by Understanding Molecular-Level Interactions and Transport Mechanisms. *Chem. Sci.* **2023**, *14* (4), 751– 770. https://doi.org/10.1039/D2SC04920A.
- 301 (6) Verbeke, R.; Gómez, V.; Koschine, T.; Eyley, S.; Szymczyk, A.; Dickmann, M.; Stimpel-302 Lindner, T.; Egger, W.; Thielemans, W.; Vankelecom, I. F. J. Real-Scale Chlorination at

- PH4 of BW30 TFC Membranes and Their Physicochemical Characterization. *J. Membr.*Sci. **2018**, 551, 123–135. https://doi.org/10.1016/j.memsci.2018.01.019.
- Verbeke, R.; Davenport, D. M.; Stassin, T.; Eyley, S.; Dickmann, M.; Cruz, A. J.; Dara, P.;
  Ritt, C. L.; Bogaerts, C.; Egger, W.; Ameloot, R.; Meersschaut, J.; Thielemans, W.;
  Koeckelberghs, G.; Elimelech, M.; Vankelecom, I. F. J. Chlorine-Resistant Epoxide-Based
  Membranes for Sustainable Water Desalination. *Environ. Sci. Technol. Lett.* 2021, 8 (9),
  818–824. https://doi.org/10.1021/acs.estlett.1c00515.
- (8) Verbeke, R.; Gómez, V.; Vankelecom, I. F. J. Chlorine-Resistance of Reverse Osmosis
   (RO) Polyamide Membranes. *Prog. Polym. Sci.* 2017, 72, 1–15.
   https://doi.org/10.1016/j.progpolymsci.2017.05.003.
- Werber, J. R.; Deshmukh, A.; Elimelech, M. The Critical Need for Increased Selectivity,
   Not Increased Water Permeability, for Desalination Membranes. *Environ. Sci. Technol. Lett.* 2016, 3 (4), 112–120. https://doi.org/10.1021/acs.estlett.6b00050.
- (10) Jung, B.; Kim, C. Y.; Jiao, S.; Rao, U.; Dudchenko, A. V.; Tester, J.; Jassby, D. Enhancing
   Boron Rejection on Electrically Conducting Reverse Osmosis Membranes through Local
   Electrochemical PH Modification. *Desalination* 2020, 476, 114212.
   https://doi.org/10.1016/j.desal.2019.114212.
- (11) Fujioka, T.; Oshima, N.; Suzuki, R.; Khan, S. J.; Roux, A.; Poussade, Y.; Drewes, J. E.;
  Nghiem, L. D. Rejection of Small and Uncharged Chemicals of Emerging Concern by
  Reverse Osmosis Membranes: The Role of Free Volume Space within the Active Skin
  Layer. Sep. Purif. Technol. 2013, 116, 426–432.
  https://doi.org/10.1016/j.seppur.2013.06.015.
- (12) Nguyen, D. T.; Lee, S.; Lopez, K. P.; Lee, J.; Straub, A. P. Pressure-Driven Distillation
   Using Air-Trapping Membranes for Fast and Selective Water Purification. *Sci. Adv.* 2023.
- (13) Lee, J.; Karnik, R. Desalination of Water by Vapor-Phase Transport through Hydrophobic
   Nanopores. J. Appl. Phys. 2010, 108 (4), 044315. https://doi.org/10.1063/1.3419751.
- (14) Deshmukh, A.; Boo, C.; Karanikola, V.; Lin, S.; Straub, A. P.; Tong, T.; Warsinger, D. M.;
   Elimelech, M. Membrane Distillation at the Water-Energy Nexus: Limits, Opportunities,
   and Challenges. *Energy Environ. Sci.* 2018, 11 (5), 1177–1196.
   https://doi.org/10.1039/C8EE00291F.
- 333 (15) Liu, W.; Wang, R.; Straub, A. P.; Lin, S. Membrane Design Criteria and Practical Viability 334 of Pressure-Driven Distillation. *Environ. Sci. Technol.* **2023**, *57* (5), 2129–2137. 335 https://doi.org/10.1021/acs.est.2c07765.
- (16) Lopez, K. P.; Wang, R.; Hjelvik, E. A.; Lin, S.; Straub, A. P. Toward a Universal
   Framework for Evaluating Transport Resistances and Driving Forces in Membrane-Based
   Desalination Processes. *Sci. Adv.* 2023, 9 (1), eade0413.
   https://doi.org/10.1126/sciadv.ade0413.
- (17) Chen, W.; Chen, S.; Liang, T.; Zhang, Q.; Fan, Z.; Yin, H.; Huang, K.-W.; Zhang, X.; Lai,
  Z.; Sheng, P. High-Flux Water Desalination with Interfacial Salt Sieving Effect in
  Nanoporous Carbon Composite Membranes. *Nat. Nanotechnol.* 2018, *13* (4), 345–350.
  https://doi.org/10.1038/s41565-018-0067-5.
- (18) Gong, D.; Yin, Y.; Chen, H.; Guo, B.; Wu, P.; Wang, Y.; Yang, Y.; Li, Z.; He, Y.; Zeng, G.
   Interfacial Ions Sieving for Ultrafast and Complete Desalination through 2D Nanochannel
   Defined Graphene Composite Membranes. *ACS Nano* 2021, *15* (6), 9871–9881.
   https://doi.org/10.1021/acsnano.1c00987.

- (19) Perreault, F.; Jaramillo, H.; Xie, M.; Ude, M.; Nghiem, L. D.; Elimelech, M. Biofouling
   Mitigation in Forward Osmosis Using Graphene Oxide Functionalized Thin-Film
   Composite Membranes. *Environ. Sci. Technol.* 2016, 50 (11), 5840–5848.
   https://doi.org/10.1021/acs.est.5b06364.
- 352 (20) Bar-Zeev, E.; Perreault, F.; Straub, A. P.; Elimelech, M. Impaired Performance of Pressure-353 Retarded Osmosis Due to Irreversible Biofouling. *Environ. Sci. Technol.* **2015**, *49* (21), 354 13050–13058. https://doi.org/10.1021/acs.est.5b03523.
- Yao, Y.; Zhang, P.; Jiang, C.; DuChanois, R. M.; Zhang, X.; Elimelech, M. High
   Performance Polyester Reverse Osmosis Desalination Membrane with Chlorine Resistance.
   Nat. Sustain. 2021, 4 (2), 138–146. https://doi.org/10.1038/s41893-020-00619-w.
- 358 (22) Deshmukh, A.; Lee, J. Membrane Desalination Performance Governed by Molecular 359 Reflection at the Liquid-Vapor Interface. *Int. J. Heat Mass Transf.* **2019**, *140*, 1006–1022. 360 https://doi.org/10.1016/j.ijheatmasstransfer.2019.06.044.
- 361 (23) Alkhudhiri, A.; Darwish, N.; Hilal, N. Membrane Distillation: A Comprehensive Review. 362 *Desalination* **2012**, *287*, 2–18. https://doi.org/10.1016/j.desal.2011.08.027.
- 363 (24) Straub, A. P.; Yip, N. Y.; Lin, S.; Lee, J.; Elimelech, M. Harvesting Low-Grade Heat
   364 Energy Using Thermo-Osmotic Vapour Transport through Nanoporous Membranes. *Nat. Energy* 2016, *I* (7), 1–6. https://doi.org/10.1038/nenergy.2016.90.
- 366 (25) Yekta-Fard, M.; Ponter, A. B. The Influences of Vapor Environment and Temperature on 367 the Contact Angle-Drop Size Relationship. *J. Colloid Interface Sci.* **1988**, *126* (1), 134–140. 368 https://doi.org/10.1016/0021-9797(88)90107-5.
- 369 (26) Lee, S.; Straub, A. P. Opportunities for High Productivity and Selectivity Desalination via 370 Osmotic Distillation with Improved Membrane Design. *J. Membr. Sci.* **2020**, *611*, 118309. 371 https://doi.org/10.1016/j.memsci.2020.118309.
- Zhang, Y.; Zhao, P.; Li, J.; Hou, D.; Wang, J.; Liu, H. A Hybrid Process Combining
   Homogeneous Catalytic Ozonation and Membrane Distillation for Wastewater Treatment.
   *Chemosphere* 2016, 160, 134–140. https://doi.org/10.1016/j.chemosphere.2016.06.070.
- (28) Merle, T.; Pronk, W.; von Gunten, U. MEMBRO3X, a Novel Combination of a Membrane
   Contactor with Advanced Oxidation (O3/H2O2) for Simultaneous Micropollutant
   Abatement and Bromate Minimization. *Environ. Sci. Technol. Lett.* 2017, 4 (5), 180–185.
   https://doi.org/10.1021/acs.estlett.7b00061.
- (29) Karami, P.; Khorshidi, B.; Soares, J. B. P.; Sadrzadeh, M. Fabrication of Highly Permeable and Thermally Stable Reverse Osmosis Thin Film Composite Polyamide Membranes. *ACS Appl. Mater. Interfaces* 2020, *12* (2), 2916–2925. https://doi.org/10.1021/acsami.9b16875.
- 382 (30) Du, Y.; Xie, L.; Wang, Y.; Xu, Y.; Wang, S. Optimization of Reverse Osmosis Networks with Spiral-Wound Modules. *Ind. Eng. Chem. Res.* **2012**, *51* (36), 11764–11777. https://doi.org/10.1021/ie300650b.
- 385 (31) Kim, S.-J.; Oh, B. S.; Yu, H.-W.; Kim, L. H.; Kim, C.-M.; Yang, E.-T.; Shin, M. S.; Jang, A.; Hwang, M. H.; Kim, I. S. Foulant Characterization and Distribution in Spiral Wound Reverse Osmosis Membranes from Different Pressure Vessels. *Desalination* **2015**, *370*, 44–52. https://doi.org/10.1016/j.desal.2015.05.013.
- (32) Lee, S.; Straub, A. P. Analysis of Volatile and Semivolatile Organic Compound Transport in Membrane Distillation Modules. *ACS EST Eng.* 2022, 2 (7), 1188–1199.
   https://doi.org/10.1021/acsestengg.1c00432.